Atmos. Meas. Tech. Discuss., doi:10.5194/amt-2016-51, 2016
Manuscript under review for journal Atmos. Meas. Tech.
Published: 29 February 2016

Atmospheric Measurement Techniques Discussions

Measurement of OH reactivity by laser flash photolysis coupled with laser-induced fluorescence spectroscopy

Daniel Stone[1], Lisa K. Whalley[1,2], Trevor Ingham[1,2], Peter M. Edwards[1,*], Daniel R. Cryer[1], Charlotte A. Brumby[1], Paul W. Seakins[1,2] and Dwayne E. Heard[1,2]

[1] *School of Chemistry, University of Leeds, Leeds, LS2 9JT, UK*

[2] *National Centre for Atmospheric Science (NCAS), University of Leeds, Leeds, LS2 9JT, UK*

**now at Wolfson Atmospheric Chemistry Laboratories, Department of Chemistry, University of York, Heslington, York, YO10 5DD*

Abstract

OH reactivity (k'_{OH}) is the total pseudo-first-order loss rate coefficient describing the removal of OH radicals to all sinks in the atmosphere, and is the inverse of the chemical lifetime of OH. Measurements of ambient OH reactivity can be used to discover the extent to which measured OH sinks contribute to the total OH loss rate. Thus, OH reactivity measurements enable determination of the comprehensiveness of measurements used to predict air quality and ozone production, and, in conjunction with measurements of OH radical concentrations, to assess our understanding of OH production rates.

In this work, we describe the design and characterisation of an instrument to measure OH reactivity using laser flash photolysis coupled to laser-induced fluorescence (LFP-LIF) spectroscopy. The LFP-LIF technique produces OH radicals in isolation, and thus minimises potential interferences in OH reactivity measurements owing to the reaction of HO_2 with NO which can occur if HO_2 is co-produced with OH in the instrument. Capabilities of the instrument for ambient OH reactivity measurements are illustrated by data collected during field campaigns in London, UK, and York, UK.

We also present the coupling and characterisation of the LFP-LIF instrument to an atmospheric chamber for measurements of OH reactivity during simulated experiments, and provide suggestions for future improvements to OH reactivity LFP-LIF instruments.

1. Introduction

OH radicals dominate atmospheric oxidation chemistry, controlling the lifetimes of most primary pollutants and greenhouse gases emitted into the atmosphere, including methane, CO, volatile organic compounds (VOCs), NO_2 and SO_2, whilst also contributing to the production of secondary pollutants such as ozone, sulphuric acid and secondary organic aerosol (SOA). Appreciation of the factors controlling atmospheric OH radical concentrations is thus essential to understanding the processing and fate of trace species in the atmosphere, and to our ability to understand and predict air quality and climate change. Moreover, the short chemical lifetimes of the OH radical and the closely related HO_2 radical make OH and HO_2 ideal species for testing the chemical mechanisms used in atmospheric models since their concentrations are controlled by in situ chemistry alone and are not influenced by transport processes. However, model simulations of OH concentrations require calculation of both OH production and loss rates, and there is potential for agreement between modelled and observed OH concentrations based on opposing errors in the production and loss terms.

Observations of OH radical concentrations made in conjunction with measurements of OH reactivity (k'_{OH}), the total loss rate of OH and the inverse of the OH chemical lifetime (τ_{OH}), thus provide a means to separate the production

Atmos. Meas. Tech. Discuss., doi:10.5194/amt-2016-51, 2016
Manuscript under review for journal Atmos. Meas. Tech.
Published: 29 February 2016

Atmospheric Measurement Techniques Discussions

and loss terms for OH, enabling a more robust test of our understanding of OH radical concentrations and of atmospheric oxidation chemistry. In addition, comparison of measured OH reactivity with calculated OH reactivity, based on observed concentrations of OH sinks and known rate coefficients for their reactions with OH (Equation 3), also provides an indication of the presence and importance of unmeasured OH sinks.

$$-d[OH]/dt = \Sigma k_x[X][OH] \quad \text{(Equation 1)}$$

$$= k_{OH}'[OH] \quad \text{(Equation 2)}$$

$$k_{OH}' = \Sigma k_x[X] \quad \text{(Equation 3)}$$

where k_x is the rate coefficient for reaction of OH with species X and k'_{OH} is the OH reactivity (the pseudo-first-order rate coefficient for reaction of OH with all reaction partners present). Finally, using both [OH] and k_{OH}' to determine $-d[OH]/dt$ experimentally, it is possible to evaluate the completeness of our knowledge of OH sources, which when added together should equal $+d[OH]/dt$ if the steady-state budget is closed (Martinez et al., 2003; Whalley et al., 2011; Fuchs et al., 2013; Lu et al., 2013).

Measurements of OH reactivity in the atmosphere have been made by three different techniques – the flow tube technique, the laser flash photolysis technique and the comparative reactivity method, with all three methods relying on production of above ambient concentrations of OH radicals and monitoring of the OH decay rate, either directly or indirectly. The flow tube method typically generates OH radicals at the tip of a sliding injector by photolysis of water vapour (R1) using a mercury vapour lamp, also resulting in production of HO_2 radicals (R2).

$$H_2O + h\nu \rightarrow H + OH \quad \text{(R1)}$$

$$H + O_2 (+M) \rightarrow HO_2 (+M) \quad \text{(R2)}$$

The OH radical signal is monitored downstream of the injector after mixing with a flow of ambient air in the main tube. By changing the position of the sliding injector relative to the point at which OH is detected it is possible to vary the mixing time of OH with the ambient air, and thus to determine the total loss rate for OH in the flow tube. However, the technique has a number of disadvantages. The time resolution of measurements made by the flow tube method is relatively poor, owing to the need to measure OH signals at a number of different injector positions to obtain a kinetic profile, during which time the ambient OH reactivity could show significant variability, although Mao et al. (2009) overcome this issue for airborne measurements of OH reactivity by reducing the number of time points used to determine the OH decay rate. The flow rates of sampled air in the flow tube method are relatively high (~ 300-900 slm (standard litres per minute)), with turbulent flow conditions leading to high wall loss rates of OH in the flow tube and relatively high uncertainties in determinations of OH reactivity owing to uncertainties in the wall loss rates. Knowledge of the flow velocity in the flow tube, requiring direct measurement or knowledge of the flow regime, total flow rate and cross-section of the flow tube, is also needed to convert the distance over which OH and ambient air are mixed to reaction time, and can lead to uncertainties in the contact time between OH and reactants in ambient air. A significant disadvantage of the flow tube method is the generation of equal concentrations of OH and HO_2 following photolysis of water vapour at the tip of the sliding injector (reactions R1-R2), leading to the potential for production of OH in the flow tube on the timescale of the experiment owing to the reaction of HO_2 with ambient NO (R3).

$$HO_2 + NO \rightarrow OH + NO_2 \quad \text{(R3)}$$

The production of OH from R3 reduces the observed decay rate of OH in the flow tube, and measurements of OH reactivity using the flow tube method thus also require simultaneous measurements of ambient NO concentrations in order to correct for interferences from HO_2 + NO, which can be quite significant. For example, for 75 ppb NO, a typical rush hour mixing ratio in Mexico City, a correction factor of ~1.7 was required to account for the production of OH from HO_2 + NO within the flow tube (Shirley et al., 2006).

Atmos. Meas. Tech. Discuss., doi:10.5194/amt-2016-51, 2016
Manuscript under review for journal Atmos. Meas. Tech.
Published: 29 February 2016

Atmospheric Measurement Techniques Discussions

In the comparative reactivity technique, a reactive molecule not usually present in air, typically pyrrole, is entrained in a gas flow and the rate of its decay owing to reaction with artificially high concentrations of OH is measured in 'zero' air and ambient air by proton transfer mass spectrometry (PTR-MS), or gas chromatography with mass spectrometry (GC-MS) or photoionisation detection (GC-PID). Comparison of the rates of decay of the molecule in 'zero' air and ambient air enables determination of the competition between the reaction of OH with the known concentration of the reactive molecule and the reaction of OH with sinks in ambient air, thus enabling measurement of the ambient OH reactivity. Absolute measurement of the physical loss rate of OH is not required for the technique, and the limit of detection of comparative reactivity instruments is determined by the sensitivity to changes in the signal corresponding to the concentration of the reactive species. However, OH radicals are typically produced in comparative reactivity instruments through reactions R1-R2, in a similar manner to that used in flow tube instruments and thus also producing high concentrations of HO_2. Interferences resulting from OH production from HO_2 + NO are thus also potentially problematic for comparative reactivity instruments and knowledge of HO_2 and NO concentrations are required to correct for any interferences. In addition, the amount of OH produced is dependent on humidity, and it is essential to ensure constant humidity between measurements made in 'zero' air and those made in ambient air, with significant corrections often necessary to account for any differences (Michoud et al., 2015).

The laser flash photolysis technique produces OH in isolation via laser photolysis of O_3, typically at a wavelength of 266 nm, followed by reaction of $O(^1D)$ with ambient H_2O (reactions R4-R5):

$$O_3 + h\nu\ (\lambda{=}266nm) \rightarrow O_2 + O(^1D) \quad (R4)$$

$$O(^1D) + H_2O \rightarrow 2\ OH \quad (R5)$$

The production of OH without initial co-production of HO_2 minimises potential interferences from HO_2 + NO and renders the flash photolysis technique more suitable to high NO_x (NO_x = NO + NO_2) environments. The laser flash photolysis method also has the advantage that the production of OH radicals is uniform throughout the reaction cell, minimising the risk of poor mixing which is potentially problematic for the flow tube and comparative reactivity techniques. Flow rates of sampled air are typically lower for the laser flash photolysis instruments (~ 12-20 slm) (Sadanaga et al., 2004a) than for those using flow tubes (~ 300-900 slm) (Kovacs and Brune, 2001; Kovacs et al., 2003; Ingham et al., 2009; Hansen et al., 2014), and the resulting laminar flow of gas reduces contact of the gas with the walls of the instrument, thus reducing the physical loss rate of OH and associated uncertainties. Although averaging of data is often required to improve signal-to-noise, a significant advantage of the laser flash photolysis technique is the ability to measure ambient OH reactivity in 'real-time' through time-resolved measurements of the OH decay following photolysis. The technique has the potential for significantly enhanced time resolution, both in terms of the number of time points obtained during the decay of OH, and the averaging time over which the data are reported, compared to the flow tube or comparative reactivity methods.

The first atmospheric measurements of total OH reactivity were made at an urban background site in Nashville, TN, USA, in summer 1999 using the flow tube technique (Kovacs and Brune, 2001; Kovacs et al., 2003). Calculations of OH reactivity, using VOC measurements co-located with the reactivity measurements, underestimated the total observed reactivity by ~30 % on average owing to unmeasured or unknown VOCs and VOC oxidation products (Kovacs et al., 2003). Subsequent measurements at an urban background site in New York, NY, USA, were, on average, within 10 % of the calculated reactivity in summer 2001 (Ren et al., 2003), but were underestimated by 30-40 % during morning and evening rush hours in winter (Ren et al., 2006a). Significant underestimation of the measured OH reactivity in the morning rush hour was also reported for observations in the Mexico City Metropolitan Area (MCMA), with the observed reactivity reaching 120 s^{-1} (Shirley et al., 2006). High OH reactivity has also been observed in Paris during the MEGAPOLI campaign in 2010, with k_{OH} reaching 130 s^{-1} for continental air masses and calculations underestimating the reactivity by up to 75 % (Dolgorouky et al., 2012). Reactivity measurements in Tokyo were underestimated in summer, spring and autumn, but reproduced to within 5 % in winter, with the reactivity correlating well with NO_x throughout the year (Sadanaga et al., 2004b; Yoshino et al., 2006; Chatani et al.,

Atmos. Meas. Tech. Discuss., doi:10.5194/amt-2016-51, 2016
Manuscript under review for journal Atmos. Meas. Tech.
Published: 29 February 2016

Atmospheric Measurement Techniques Discussions

2009; Yoshino et al., 2012). Aircraft measurements of OH reactivity have also shown that reactivity tends to decrease with altitude, with discrepancies between observed and calculated reactivity most pronounced at altitudes up to 2 km and tending towards agreement at altitudes above 4 km (Mao et al., 2009).

Flow tube measurements at an urban site in Houston, US, during the TEXAQS2000 and TRAMP2006 campaigns (Mao et al., 2010) and at a forested site at Whiteface Mountain, NY, USA (Ren et al., 2006b), were well reproduced by model calculations. However, measurements made at a coastal site in Norfolk, UK, typically characterised by relatively 'clean' air were significantly underestimated and attributed to the presence of numerous high molecular mass VOCs at low concentrations which were not included in the VOC measurement suite (Lee et al., 2009; Ingham et al., 2009). The presence of unmeasured VOCs was also indicated for the PROPHET 2000 campaign at a forested site in Michigan, USA, during which the measured OH reactivity was underestimated by ~50 % on average, with the 'missing' OH reactivity exhibiting a strong temperature dependence potentially resulting from temperature-dependent emissions of unmeasured biogenic VOCs (Di Carlo et al., 2004). Uncertainties in emissions and chemistry of biogenic VOCs, particularly in the oxidation chemistry of isoprene and its oxidation products, have also been responsible for underpredictions of observed OH reactivity in forested regions in Suriname (Sinha et al., 2008) and Borneo (Whalley et al., 2011; Edwards et al., 2013). Model calculations of OH reactivity in Borneo underestimated the observed diurnal mean reactivity by 30 %, and indicated that uncertainties in the chemistry and deposition rates of secondary oxidation products could potentially explain the observed reactivity without the need for additional primary VOC emissions, and that at least 50 % of the carbon-containing compounds which react with OH were not measured (Edwards et al., 2013). Biogenic VOCs also dominated the daytime OH reactivity in the Pearl River Delta region, China, with isoprene and its oxidation products comprising ~40 % of the total OH reactivity in the afternoon and observed reactivity underestimated by ~50 % when calculated from measured OH sinks but reproduced by model calculations considering the contributions from secondary oxidation products (Lou et al., 2010). However, observations of OH reactivity in a forested region in Colorado, USA, during the BEACHON-SRM08 campaign were underestimated by model calculations (~ 30 %), with the dominant VOCs found to be 2-methyl-3-buten-2-ol (MBO) and monoterpenes (Nakashima et al., 2014).

Using a branch enclosure technique, Kim et al. (2011) demonstrated that underestimations of observed OH reactivity at the PROPHET field site, Michigan, USA, during the 2009 CABINEX campaign were related to oxidation products of known and measured biogenic VOCs, rather than to unknown or unmeasured primary VOC emissions. Model calculations were able to reproduce the CABINEX OH reactivity observations below the forest canopy, but discrepancies were apparent above the canopy, indicating the presence of unmeasured trace gases above the forest canopy (Hansen et al., 2014). Model calculations and experiments using the comparative reactivity method at a forested site in Finland also observed differences between OH reactivity measured in the forest canopy and above the canopy (Mogensen et al., 2011; Nolscher et al., 2012). While the in-canopy reactivity was typically higher than the above canopy reactivity, transport of wildfire plumes to the site significantly increased the above canopy reactivity, increasing it above the in-canopy level and increasing the 'missing' reactivity above the canopy from 58 % for 'normal' conditions to 73 % for periods impacted by transported pollution (Nolscher et al., 2012).

OH reactivity measurements have also been used to determine ozone production rates in southwestern Spain during the DOMINO campaign (Sinha et al., 2012) and in London during the ClearfLo campaign (Whalley et al., 2015), and have been used in laboratory studies to assess our understanding of combustion systems (Nakashima et al., 2010) and atmospheric isoprene oxidation mechanisms (Nakashima et al., 2012; Nolscher et al., 2014).

Measurements of OH reactivity thus have a number of applications, and can be used to improve our understanding of atmospheric composition and chemistry. In this work we present the design and characterisation of an instrument using laser flash photolysis coupled with laser-induced fluorescence (LFP-LIF) to measure OH reactivity in the field and in chamber experiments.

Atmos. Meas. Tech. Discuss., doi:10.5194/amt-2016-51, 2016
Manuscript under review for journal Atmos. Meas. Tech.
Published: 29 February 2016

Atmospheric Measurement Techniques Discussions

2. Experimental

A schematic of the OH reactivity instrument is given in Figure 1. The instrument comprises a reaction cell (described in Section 2.1) and a detection cell (described in Section 2.2), with the two cells typically situated approximately 5 m above ground level on the roof of a shipping container housing the FAGE mobile laboratory during ambient measurements.

2.1 Reaction Cell

The reaction cell consists of a cylindrical stainless steel tube of 50 mm internal diameter and 85 cm in length. Ambient air is drawn through a stainless steel sampling line (50 mm internal diameter and 20 cm in length), enters the reaction cell at 90^{o} to the air flow in the tube, and is drawn along the tube by an extractor fan mounted on the exit arm situated immediately prior to the OH detection cell (Section 2.2). The fan speed determines the flow rate of gas in the reaction cell, and is set to ensure a laminar flow of air through the cell with a Reynold's number less than 2300. The flow rate of gas, determined by measurement of the flow velocity using a hot-wire anemometer (TSI Air velocity transducer 8455-150) or set by calibrated mass flow controllers during laboratory experiments (Sections 4, 6 & 7) and measurements of instrument zeroes (Section 3.1), was in the range 12 to 14 slm, giving a residence time of 7 to 8 s in the reaction cell and a Reynold's number of ~ 360 (Equation 4).

$$R_e = \rho v D / \mu \qquad \text{(Equation 4)}$$

where R_e is the Reynold's number, ρ is the density of the gas, v is the mean gas velocity, D is the diameter of the flow tube and μ is the dynamic viscosity of the gas.

Production of OH radicals within the reaction cell is achieved by the 266 nm laser photolysis of O_3 in the presence of water vapour (reactions R4-R5). A flashlamp pumped Nd:YAG laser (Big Sky Laser CFR 200, Quantel USA) is used to generate laser light at 1064 nm, which is frequency doubled to 532 nm (lithium triborate, LiB_3O_5, doubling crystal) and then frequency doubled to generate the fourth harmonic 266 nm radiation (caesium lithium triborate, $CsLiB_6O_{10}$, doubling crystal) with pulse energies of ~ 50 mJ, pulse length 8 ns, and beam diameter of 6.35 mm. The laser is operated with a Q-switch to modulate the intracavity losses and maximise the pulse energy.

The 266 nm laser head is situated adjacent to the reaction cell in order to minimise the footprint of the instrument when used in the field. The laser head is powered, controlled and water cooled by an Integrated Cooler and Electronics unit (Big Sky Laser ICE450, Quantel USA) which is housed within the FAGE shipping container and powered via an uninterruptible power supply (APC 1000VA, American Power Conversion by Schneider Electric).

Laser light exiting the laser head is directed into the reaction cell using two dielectrically coated 266 nm turning mirrors of 1" diameter (Thorlabs, NB1-K04). Immediately prior to the reaction cell, the 266 nm beam is expanded to a diameter of ~10 mm by a telescope incorporating a plano-concave lens (Thorlabs LC4252, focal length = -30 mm) and a plano-convex lens (Thorlabs LA4148, focal length = 50 mm) housed in a lens tube (SM1M20, Thorlabs) to increase the photolysis volume within the reaction cell. The photolysis laser enters the reaction cell through a fused silica window, initiating OH radical production.

Typically, there is sufficient production of OH in the instrument from reactions R4-R5 at ambient concentrations of O_3 and water vapour in order to measure a temporal decay of OH. At low ambient concentrations of O_3 (< 10 ppb) or during laboratory tests (Sections 4, 6 and 7) and measurement of instrument zeroes (Section 3), the OH radical concentration in the reaction cell is increased by passing a small flow (0.5 slm) of humidified ultra-high purity air (BTCA 178, BOC Special Gases) across a low pressure Hg vapour lamp and mixed with the main sampled air flow (12 – 14 slm) in the inlet to the reaction cell. The mixing ratio of ozone in the reaction cell is increased by ~ 50 ppb by this method (measured by an ozone analyser (Thermo Environmental Instruments Inc., 49C O_3 Analyser) situated at the end of the reaction cell during laboratory tests). Given knowledge of the rate coefficient for reaction of OH with O_3 (k_{OH+O3} =7.3 × 10^{-14} cm^3 s^{-1}, Atkinson et al., 2004), the chemical loss of OH resulting from the addition of 50 ppb O_3 is <

Atmos. Meas. Tech. Discuss., doi:10.5194/amt-2016-51, 2016
Manuscript under review for journal Atmos. Meas. Tech.
Published: 29 February 2016

Atmospheric Measurement Techniques Discussions

0.1 s^{-1} at 298 K, and any loss of VOCs in the reaction cell through reaction with ozone is extremely small given the reaction times involved.

2.2 OH Detection Cell

OH radicals in the reaction cell are monitored by laser-induced fluorescence (LIF) using the fluorescence assay by gas expansion (FAGE) technique. The LIF-FAGE detection cell has been described previously in detail (Ingham et al., 2009), thus only a brief description will be given here.

Initial experiments were conducted with the detection cell situated midway along the reaction cell (Figure 1a), and sampling at 90° to the direction of air flow along the reaction cell, in a similar design to that described by Sadanaga et al. (2004a) and Lou et al. (2010). However, the observed OH decays in such a configuration displayed biexponential behaviour, comprising a fast initial decay followed by a slower decay representative of the expected OH reactivity, as observed in previously described instruments (Sadanaga et al., 2004a; Lou et al., 2010). In this configuration, the photolysis laser is aligned such that the beam passes across the inlet to the detection cell without hitting the inlet (as shown in Figure 1a). The air sampled in to the detection cell thus likely contains air that has experienced the photolysis laser (containing elevated OH concentrations) and air that has not experienced the photolysis laser (containing only ambient OH concentrations), with this mixing of air potentially leading to an apparent increase in the initial OH decay rate owing to dilution of the air containing elevated OH concentrations with air containing lower OH concentrations. Once mixing of the air having experienced the photolysis laser with that outside the beam diameter has occurred sufficiently to give uniform OH concentrations in the reaction cell the observed OH decay will result from the chemical losses in the instrument, leading to biexponential decays. Such biexponential behaviour has been attributed to similar effects of non-homogeneous spatial distributions of OH near the inlet to the detection cell (Lou et al., 2010) and to local heating and turbulence of the gas flow caused by the photolysis laser (Sadanaga et al., 2004a). A comparison between sampling at 90° to the direction of air flow along the reaction cell and sampling along the axis of the direction of air flow from the centre of the reaction cell has been reported previously (Amedro et al., 2012), with different fitting procedures required to extract the OH reactivity for the different instrument configurations attributed to differences in physical effects such as diffusion which were more significant when sampling at 90° (Amedro et al., 2012).

Subsequent experiments in this work (including all those described below) were performed with the detection cell situated at the end of the reaction cell along the same axis as the direction of air flow to sample air directly from the centre of the reaction cell, as shown in Figure 1b. This configuration reduces the chance of sampling air into the detection cell that has not experienced the photolysis laser beam, and thus reduces the impact of physical effects such as diffusion. The observed OH signals in this instrument configuration are described by a single exponential decay, although biexponential decays can still be obtained if the photolysis laser is not correctly aligned along the axis of the reaction cell.

Air is sampled from the centre of the reaction cell through a pinhole of 0.8 mm diameter and 0.5 mm thickness into the aluminium detection cell, which consists of three orthogonal axes and is black anodised to minimise light scattering within the cell. The pressure in the cell is measured by a capacitance manometer (Sensotec Z/606-01ZA) and is maintained at ~ 1.5 Torr by a roots blower backed by a rotary pump (Leybold Vacuum SV200/WAU1001), resulting in an air flow of approximately 4 slm and a supersonic expansion of the air as it is drawn through the pinhole.

The probe laser consists of a Nd:YAG pumped Ti:Sapphire laser (Photonics Industries) which generates broadband radiation in the range 690-1000 nm. A diffraction grating is used to select radiation with λ = 924 nm, which is frequency tripled through generation of the second harmonic at 462 nm followed by sum-frequency mixing of the 462 nm radiation with that at 924 nm to produce the 308 nm light with a pulse repetition frequency (PRF) of 5 kHz, pulse length (full width half maximum (FWHM)) of 35 ns, laser line width (FWHM) of 0.065 cm^{-1} and beam diameter of ~ 3mm (Bloss et al., 2003).

Atmos. Meas. Tech. Discuss., doi:10.5194/amt-2016-51, 2016
Manuscript under review for journal Atmos. Meas. Tech.
Published: 29 February 2016

Atmospheric Measurement Techniques Discussions

A reference fluorescence cell containing a heated nichrome wire filament and humidified air at ~2 Torr to produce a constant stable source of OH radicals from dissociation of water vapour is used to facilitate tuning the probe laser to the precise wavelength required for the desired OH transition. Approximately 1 mW of the 308 nm laser light is used for this purpose, with ~9 mW used to make measurements of OH reactivity and a further ~13 mW remaining to make measurements of ambient OH, HO_2 and RO_2 concentrations in a separate instrument (see, for example, Whalley et al., 2015).

The probe laser, reference cell and pumps are all situated inside the shipping container. The ~9 mW of the 308 nm laser light used to measure OH reactivity is passed to the detection cell on the roof of the shipping container via an anti-reflective coated optical fibre with an angled and polished end (Oz Optics, QMMJ-55-UVVIS-200/240-3-30-AR2-SP, length = 30 m) through a baffled side-arm at 90° to the air flow. The probe laser light exits the detection cell through a baffled side-arm and is directed onto a photodiode (New Focus Large Area Photoreceiver 2032) to measure the laser power to enable normalisation of fluorescence signals for fluctuations in laser power. For a recent intercomparison at the SAPHIR chamber, the OH reactivity instrument, comprising the reactor flowtube and OH fluorescence and associated equipment was placed in the shipping container itself.

Fluorescence from electronically excited OH radicals resulting from excitation of the $Q_1(1)$ $A^2\Sigma^+$ (v'=0) – $X^2\Pi_{3/2}$ (v''=0) transition at 308 nm is collimated by a symmetrical biconvex collimating lens (Melles-Griot, focal length = 50 mm at λ = 546.1 nm, diameter = 50 mm) and focused onto the photocathode of a channeltron photomultiplier tube (PMT) (Perkin Elmer C 943P) by two plano-convex focusing lenses (UQG Optics Ltd., focal length = 75 mm at λ = 250 nm, diameter = 50 mm). A narrow band UV interference filter (Barr Associates Inc., FWHM bandwidth of 8 ± 1.6 nm centred at 309 ± 1 nm with a peak transmission of > 50 % at 308 nm and a blocking factor of 10^6 at other wavelengths) is situated between the excitation region in the detection cell and the PMT to minimise detection of scattered solar photons. The solid angle from which fluorescence is collected is effectively doubled through the use of a spherical concave mirror coated for high UV reflectance which is mounted in the detection cell opposite the side-arm bearing the PMT. Discrete photon signals on the PMT are processed using a multi-channel scaler photon counting card (Becker and Hickl, PMS 400, minimum bin width of 250 ns) in the computer used to control the instrument.

2.3 Instrument Control

A digital delay pulse generator (Stanford Research Systems DG535) produces a 5 kHz TTL (transistor-transistor logic) pulse to trigger the Ti:Sapphire laser and a second delay generator (Stanford Research Systems DG535) which subsequently triggers the gating of the PMT detector for the reactivity instrument and a third digital delay pulse generator (Berkeley Nucleonics Corporation 555) to trigger the 266 nm photolysis laser and the photon counting card at the specified pulse repetition frequency in synchronisation with the 308 nm probe laser. A personal computer is used to automate data collection, with analogue signals from measurements of the pressure in the detection cell and the power of the 308 nm probe laser at the photodiode attached to the detection cell digitised by an A/D card (Measurement Computing, PCI-DAS 1200). Electrical power to all parts of the instrument is supplied via an uninterruptible power supply (APC 1000VA).

2.4 Data Acquisition

Data acquisition is initiated by triggering of the photon counting card, with a background signal measured for 100 ms before triggering of the 266 nm photolysis laser and production of OH in the reaction cell. To avoid saturation of the PMT resulting from detection of the 308 nm laser pulse itself, the PMT is gated off at the onset of the 308 nm laser pulse (35 ns FWHM) until ~100 ns after the laser pulse, thereby preventing detection of any reflected or scattered laser light. The fluorescence signal is typically collected for 1 µs following each 308 nm probe laser pulse. Repeated measurements of the OH fluorescence signal are taken for 900 ms following each 266 nm photolysis laser pulse, during which time the OH concentration and hence the fluorescence signal will decay to the background level. Under normal conditions this occurs within ~300 ms of the photolysis laser pulse, although this is of course dependent upon the magnitude of the OH reactivity, and may be longer. The pulse repetition frequency of the 308 nm probe

Atmos. Meas. Tech. Discuss., doi:10.5194/amt-2016-51, 2016
Manuscript under review for journal Atmos. Meas. Tech.
Published: 29 February 2016

Atmospheric Measurement Techniques Discussions

laser (5 kHz) results in measurement of the OH fluorescence signal every 200 µs throughout the measurement period. The data collection cycle, as illustrated in Figure 2 is typically repeated every 1 s. Experiments, both in the laboratory and in the field, in which the PRF of the photolysis laser was varied between 0.1 and 1 Hz showed no effect on the observed OH reactivity.

When measurements of OH reactivity are made alongside those of ambient OH concentrations, the acquisition of OH reactivity data is linked to measurements of ambient OH concentrations owing to the dual use of the 308 nm excitation laser. Under such circumstances, measurements are taken on an approximate 7 min cycle, with a 5 min 'online' period during which the 308 nm laser is at the precise wavelength to excite the OH transition, followed by a 1 min 'offline' period during which the wavelength of the laser is moved to a nearby wavelength at which the OH transition is not excited in order to enable measurement of a background signal for determination of ambient OH concentrations (see, for example, Whalley et al. (2010)). Approximately 1 min is then required to scan the laser wavelength over the OH transition to find the maximum OH fluorescence signal in the reference cell (Section 2.2). OH reactivity measurements are thus taken during the 5 min online period, and data from successive measurement cycles during each online period are co-added to improve the signal-to-noise ratio. Figure 3 shows typical OH decays derived from the co-addition of data recorded throughout 5 min online periods during the Clean Air for London (ClearfLo) campaign in summer 2012.

Measurements of OH reactivity may also be made independently of any other use of the 308 nm probe laser, in which case the timescale over which successive measurement cycles are co-added may be selected as desired, with the laser periodically scanned over the OH transition to ensure that the maximum OH signal is obtained.

2.5 Calibration of the FAGE Detection Cell

Calibration of the detection cell, although not strictly necessary for measurements of OH reactivity, is required to ensure that pseudo-first-order conditions are met in the reaction cell (i.e. combined concentrations of OH sinks are in excess over the OH concentration) and provides a means to determine any potential interferences from production of OH via ambient HO_2 + NO in the reaction cell (from ambient HO_2 which may survive the sampling inlet, and any HO_2 generated following oxidation of OH sinks in the instrument) and to monitor potential changes in instrument sensitivity with time.

The calibration procedure has been described in detail by Commane et al. (2009). Production of OH (and HO_2) is achieved through reaction R1 (and HO_2 through reaction R2) by passing a turbulent flow of humidified ultra-high purity air (BTCA 178, BOC Special Gases) across a low pressure mercury vapour lamp to photolyse water vapour at λ = 184.9 nm.

$$H_2O + h\nu\ (\lambda{=}184.9\ nm) \rightarrow H + OH \qquad (R1)$$

The concentration of OH is given by Equation 5:

$$[OH] = [H_2O]\ \sigma_{H2O}\ \varphi_{OH}\ F\ \delta t \qquad (Equation\ 5)$$

where σ_{H2O} is the absorption cross-section of H_2O at 184.9 nm $(7.1 \pm 0.2) \times 10^{-20}$ cm^2 (Cantrell et al., 1997; Creasey et al., 2000), φ_{OH} is the quantum yield for OH production (φ_{OH} = 1), F is the photon flux of the mercury lamp at 184.9 nm and δt is the residence time in the photolysis region. The product $F\ \delta t$ is determined by N_2O actinometry (Commane et al., 2009), with F varied by changing the current supplied to the lamp, and δt controlled by the flow rate of the gas used in the calibration. The concentration of water vapour in the flow is determined by diverting a small known flow of the air to a dew point hygrometer (CR4, Buck Research Instruments).

The calibration for OH was conducted over a range of mercury lamp fluxes, giving a calibration factor (C_{OH}) of $(2.13 \pm 0.27) \times 10^{-8}$ counts s^{-1} molecule^{-1} cm^3 mW^{-1} and indicating an initial OH concentration of ~10^9 cm^{-3} produced in the reaction cell by the 266 nm photolysis laser during measurements of OH reactivity in ambient air. The instrumental

Atmos. Meas. Tech. Discuss., doi:10.5194/amt-2016-51, 2016
Manuscript under review for journal Atmos. Meas. Tech.
Published: 29 February 2016

Atmospheric Measurement Techniques Discussions

limit of detection for OH radicals was determined to be ~ 10^7 cm^{-3}, enabling observation of sufficient changes in OH radical concentrations in the reaction cell to allow measurements of ambient OH reactivity.

3. Determination of OH Reactivity

The observed pseudo-first-order rate coefficient for OH loss (k_{loss}) is determined by least-squares fitting Equation 6 to the time-resolved OH decay:

$$S_{OH,t} = S_{OH,0} \exp(-k_{loss}t) + b \quad \text{(Equation 6)}$$

where $S_{OH,t}$ is the fluorescence signal at time t after firing of the 266 nm photolysis laser, $S_{OH,0}$ is the fluorescence signal at time zero (i.e. immediately following firing of the 266 nm laser and production of OH in the reaction cell), k_{loss} is the observed rate coefficient for loss of the fluorescence signal, t is the time since firing of the 266 nm photolysis laser and b is the background fluorescence signal measured by the PMT averaged for the 1 s prior to firing of the photolysis laser (typically zero). Values for $S_{OH,0}$ and k_{loss} are permitted to vary in the fitting process. Figure 3 shows typical fits of Equation 6 to measurements of OH reactivity made in ambient air.

The value for k_{loss} determined from the fit contains a contribution from $k'_{OH,obs}$, the rate coefficient for OH loss owing to chemical losses of OH in the reaction cell (the OH reactivity), and k_{phys}, the instrument 'zero' corresponding to the rate coefficient for physical losses of OH owing to diffusion out of the sampling volume and heterogeneous losses on the walls on the reaction cell. The chemical loss of OH in the reaction cell is thus given by Equation 7, and in order to determine the OH reactivity from measurements of k_{loss} it is therefore essential to characterise k_{phys} (Section 3.1).

$$k'_{OH,obs} = k_{loss} - k_{phys} \quad \text{(Equation 7)}$$

At low ambient concentrations of ozone (< 10 ppb) and in laboratory experiments (Sections 4, 6 and 7) and measurements of k_{phys}, it was necessary to add a small flow of humidified air containing a constant mixing ratio of ozone (~50 ppb) to the main air flow sampled in order to produce sufficient OH radicals in the reaction cell. This 'non-ambient' ozone added to the reaction cell results in a small loss of OH owing to the reaction of O_3 with OH, but is expected to be < 0.1 s^{-1} at 298 K (Section 2.1). However, addition of the small ozone-containing air flow (0.5 slm) to the sampled flow of ambient air (12 slm) does require a correction for the dilution of the ambient air flow, such that the OH reactivity (k'_{OH}) is given by Equation 8:

$$k'_{OH} = k'_{OH,obs} (1+f) \quad \text{(Equation 8)}$$

where f is the dilution factor of the ambient air flow, given by the ratio of the small ozone-containing flow rate to the total flow rate of the air in the reaction cell (~0.04 for the conditions used in this work). Potential errors arising from errors in measurements of k_{phys} and f have been included in overall reported errors for k'_{OH}.

3.1 Determination of k_{phys}

Determination of k_{phys} is critical to the evaluation of the true OH reactivity from observations of the total OH loss rate in the instrument (Equations 7 & 8), and requires the measurement of the OH loss rate in the absence of any chemical removal processes such that k_{loss} is equal to k_{phys}. To minimise the chemical losses of OH in the reaction cell (and thus to minimise $k'_{OH,obs}$) the loss of OH in the instrument is measured in ultra-high purity air (BTCA 178, BOC Special Gases) passed through scrubbers (Gatekeeper Gas Purifiers) to remove H_2, CO and CO_2 to sub-ppb levels. Despite the use of scrubbed ultra-high purity air, low levels of residual VOCs can remain in the air, leading to chemical losses. Such residual VOCs in the scrubbed ultra-high purity air have been quantified by gas-chromatography and their contributions (< 1 s^{-1}) to the observed OH loss subtracted.

Furthermore, humidification and addition of a small amount of O_3 to the ultra-high purity air are necessary for the production of OH in the instrument during experiments to determine k_{phys}. Approximately 50 ppb of O_3 is added to

Atmos. Meas. Tech. Discuss., doi:10.5194/amt-2016-51, 2016
Manuscript under review for journal Atmos. Meas. Tech.
Published: 29 February 2016

Atmospheric Measurement Techniques Discussions

ensure production of sufficient OH, leading to a chemical loss of < 0.1 s^{-1} at 298 K through the reaction of OH with O_3. Moreover, despite the use of purified water for humidification, obtained using a water purification system (PURELAB flex PRIPLB0163, Elga LabWater, Veolia Water Solutions & Technologies), impurities in the water can lead to significant chemical losses for OH and the components in the purification system must remain uncontaminated in order to ensure accurate determinations of k_{phys}.

Determination of k_{phys} in the laboratory and in the field for the ClearfLo campaign in London in 2012 gave an average value (1.1 ± 1.0) s^{-1} and (1.25 ± 0.42) s^{-1} for the campaign in York in 2014 (Section 5).

4. Instrumental validation via measurements of k_{OH+CO} and k_{OH+CH4}

As a real time technique, the accuracy of the time axis during which the OH decay is obtained is determined by the accuracy of the delay generators used to trigger the lasers and other delays (as described in Section 2.4 and shown in Figure 2), which should be absolute within 1 ps. Hence the method should be absolute in terms of the time separation between points in the decay. However, owing to various reasons, for example the appropriateness of the function used to fit the decay, or any recycling of OH from oxidation products (for example the reaction of HO_2 with NO), it is prudent to characterise the instrument through the use of known concentrations of reactants for which the rate coefficient with OH is also well known. In order to validate measurements of ambient OH reactivity, the well-known rate coefficients for reactions of OH with CO and CH_4 were both measured under pseudo-first-order conditions using the instrumental setup described above. Ultra-high purity air (BTCA 178, BOC Special Gases) was mixed with an excess of either CO (5 % in N_2, BOC Special Gases) or CH_4 (BOC, CP grade, 99.5%), producing a main flow of 11.5 slm with known concentrations of CO or CH_4, prior to mixing with a small flow of humidified air (0.5 slm) containing ~ 50 ppb O_3 generated by passing the air flow across a mercury vapour lamp.

Figure 4 shows the OH reactivity, determined by fitting Equation 6 to the OH decay and subtracting k_{phys} (Section 3), for a series of CO and CH_4 concentrations. The bimolecular rate coefficients for OH + CO (k_{OH+CO}) and OH + CH_4 (k_{OH+CH4}), determined at 298 K from the relationships $k'_{OH} = k_{OH+CO}[CO]$ and $k'_{OH} = k_{OH+CH4}[CH_4]$, were found to be (2.4 ± 0.2) × 10^{-13} cm^3 s^{-1} and (6.4 ± 0.6) × 10^{-15} cm^3 s^{-1}, respectively (errors are 1σ). The values for k_{OH+CO} and k_{OH+CH4} determined here are in agreement with the literature values of $(2.3 \pm^{0.6}_{0.5}) \times 10^{-13}$ cm^3 s^{-1} and $(6.4 \pm^{1.3}_{1.1}) \times 10^{-15}$ cm^3 s^{-1} at 298 K (Atkinson et al., 2004), respectively, providing confidence in measurements of ambient OH reactivity.

5. Field measurements

The laser flash photolysis OH reactivity instrument was deployed at the North Kensington measurement site (51° 31' N, 0° 12' W) during the Clean Air for London (ClearfLo) summer campaign in July and August 2012 (Bohnenstengel et al., 2014), with near-continuous measurements made from the 21st July to 18th August 2012, alongside FAGE measurements of OH, HO_2 and RO_2 radical concentrations. Measurements of O_3, CO, NO, NO_2, HONO, VOCs and aerosol mass and composition were also made at the site during the campaign.

Figure 5 shows the full time series of measured OH reactivity for the campaign. The observed reactivity was highest for air masses that had previously passed over central London (24th-27th July (Julian days 206-209) and 8th-10th August (Julian days 221-223)), with a maximum reactivity of 116 s^{-1} recorded during rush hour on 24th July 2012. Measurements taken on the 25th July 2012 (Julian day 207) are shown in Figure 6 to highlight the capability of the instrument, and the average diurnal profile for the campaign is shown in Figure 7. A peak reactivity, on average, of ~27 s^{-1} was observed during morning rush hour, with a minimum of ~15 s^{-1} during the afternoon and a second peak during evening rush hour. Detailed analysis of these data, including model calculations using the Master Chemical Mechanism constrained to observed concentrations of long-lived species, is described by Whalley et al. (2015), and the data are shown here only to highlight the instrument capability.

Atmos. Meas. Tech. Discuss., doi:10.5194/amt-2016-51, 2016
Manuscript under review for journal Atmos. Meas. Tech.
Published: 29 February 2016

Atmospheric Measurement Techniques Discussions

Field measurements of OH reactivity have also been made at a site at the University of York (53° 56' N, 1° 02' W) from the 19th May to 16th June 2014, approximately 3 km south-east of the centre of York and 2 km west of a major road, with a small wooded area immediately to the east, and thus subject to anthropogenic emissions and local biogenic emissions. Figure 8 shows the average diurnal during this period shown. The observed OH reactivity was typically lower than that observed during the ClearfLo campaign, with a maximum in the diurnal average of ~6 s^{-1}. Measurements of O_3, CO, NO, NO_2, VOCs and were also made at the site during this period, alongside measurements by a new instrument coupling an OH reactor to measurements of VOCs by gas chromatography with time of flight mass spectrometry (GC-TOFMS) to aid identification of any 'missing' OH reactivity. Detailed analysis of the results will be given in future publications.

6. Chamber measurements

The field instrument described above has also been modified in order to interface to the Highly Instrumented Reactor for Atmospheric Chemistry (HIRAC) to enable measurements of OH reactivity during VOC oxidation under controlled conditions. For complex reaction mechanisms, the oxidation pathway followed will have a characteristic time-evolution of the reactivity as secondary products are generated, and measurement of OH reactivity and comparison with a model prediction provides greater constraint for experimental determination of the mechanism.

HIRAC is a 2.25 m^3 stainless steel chamber equipped with UV photolysis lamps to initiate photochemistry and a comprehensive suite of analytical instrumentation, including gas chromatography (GC), Fourier transform infrared (FT-IR) spectroscopy, cavity ringdown spectroscopy (CRDS) and LIF-FAGE for radical measurements. Photolysis lamps within the chamber enable initiation of photochemistry, and experiments can be conducted at temperatures between 203 and 343 K and pressures up to 760 Torr (Glowacki et al., 2007; Malkin et al., 2010; Winiberg et al., 2015).

Gas is sampled from HIRAC through ½ " PTFE tubing at a flow rate of 1 slm and diluted with 5 slm of ultra-high purity air immediately on exiting the chamber, then diluted further with 9 slm of humidified ultra-high purity air and 1 slm of ultra-high purity air passed over a low pressure Hg lamp in order to generate O_3, giving a total flow of 16 slm and hence a dilution factor of 1:16. The diluted gas flow, containing ~ 45 ppb O_3, is then directed into the reaction cell of the OH reactivity instrument, with instrument operation and analysis as described in Sections 2 and 3 (including the correction of observed reactivity for dilution of sampled gas from the chamber using Equation 8, which is significant for these experiments in order to avoid measurement of high reactivities (Section 7) and to reduce the volume of gas removed from the chamber for the reactivity measurements).

Experiments were conducted to verify the sampling procedure by filling HIRAC with air containing known concentrations of a reactive gas, with a well-characterised rate coefficient for reaction with OH, followed by measurement of the OH reactivity in the chamber. Determination of the pseudo-first-order rate coefficients describing the OH loss for each of the given reactive gas concentrations in the chamber enabled determination of the bimolecular rate coefficient for reaction of the reactive gas with OH for comparison with literature values, as for experiments described in Section 4. Figure 4c shows the bimolecular plots for experiments in which the chamber was filled with *n*-butanol (*n*-C_4H_9OH) in air at total pressures of 760 Torr and temperatures of 298 K. A bimolecular rate coefficient of (8.5 ± 0.1) × 10^{-12} cm^3 s^{-1} was obtained, in comparison to the literature value of (8.5 $\pm \frac{3.5}{2.5}$) × 10^{-12} cm^3 s^{-1} (Atkinson et al., 2004), thus indicating the validity of the sampling procedure. No dependence of the observed reactivity on the total flow rate through the instrument was observed between 10 and 22 slm.

The coupling of OH reactivity measurements to chamber studies will enable detailed assessment of our understanding of the chemistry of secondary products in complex oxidation mechanisms by providing increased constraint on oxidation budgets during chamber experiments, and will be explored further in future work.

Atmos. Meas. Tech. Discuss., doi:10.5194/amt-2016-51, 2016
Manuscript under review for journal Atmos. Meas. Tech.
Published: 29 February 2016

Atmospheric Measurement Techniques Discussions

7. Effects of averaging time and future improvements to sampling

Measurements have also been made in HIRAC to investigate the effect of the averaging time on the measured OH reactivity. Figure 9 shows the observed OH reactivities, for a given set of conditions, as a function of the averaging time, showing successful measurements with an averaging time of 10 s and indicating the potential for further improvements for future integration of ambient OH reactivity observations with flux measurements.

Experiments described in this work using known concentrations of reactive gases have been able to reproduce recommended literature values for known rate coefficients, indicating the validity of the technique described here over the dynamic ranges investigated. However, recent work in Leeds has shown that, at higher reactivities, observed kinetics can be influenced by sampling issues related to the transport time of sampled gas from the pinhole nozzle to the point at which fluorescence is excited and detected in the FAGE cell, leading to underestimations of very high reactivities (Stone et al., 2016). Successful measurements in HIRAC with known concentrations of CH_4 at reactivities > 150 s^{-1} (Section 6), although scattered owing to the small number of time points over which fast decays can be measured, indicate that such effects should be minimal for the instrument described in this work, even for the highest reactivities observed during the ClearfLo campaign (> 100 s^{-1}). However, experiments incorporating OH reactivity measurements in chamber studies, such as those described in Section 6, must also ensure that the gas sampled from the chamber has been sufficiently diluted so as to avoid the measurement of high reactivities directly.

Future work will incorporate a new inlet designed to minimise the distance between the pinhole nozzle and the point of excitation fluorescence and detection, ideally such that detection occurs within the supersonic jet formed on expansion of the gas as it flows through the pinhole. The new inlet will not only increase the dynamic range over which reactivity measurements can be made, but sampling within the supersonic jet will also lead to increased signal-to-noise and enable further reductions in the averaging time required to achieve adequate signal-to-noise for measurements with high time resolution.

8. Conclusions and Outlook

In this work we present the design and characterisation of an instrument to make field and chamber measurements of OH reactivity by laser flash photolysis (LFP) coupled with laser-induced fluorescence (LIF) using the FAGE technique. The LFP-LIF reactivity instrument, its operation and data analysis have been described in detail. Ambient reactivity measurements obtained during field campaigns in London, UK, and York, UK, have been presented, and will be discussed further in future work. The instrument has also been coupled to an atmospheric chamber, and preliminary results have been shown to demonstrate the potential for reactivity measurements during future chamber experiments.

Reactivity measurements have been made using an averaging time of 10 s, indicating potential for integration of ambient OH reactivity observations with flux measurements. Future development of the instrument will increase the dynamic range over which measurements can be made and will enable reduced averaging times owing to improvements in the signal-to-noise ratio.

Acknowledgements

This work was supported by the National Environment Research Council (NERC) under grants NE/H003193/1, NE/J008990/1 and NE/L010798/1. DS is grateful to NERC for the award of an Independent Research Fellowship (NE/L010798/1). We are also grateful to the National Centre for Atmospheric Science (NCAS), which is funded by NERC, for ongoing support.

Atmos. Meas. Tech. Discuss., doi:10.5194/amt-2016-51, 2016
Manuscript under review for journal Atmos. Meas. Tech.
Published: 29 February 2016

Atmospheric Measurement Techniques Discussions

522 **Figures**

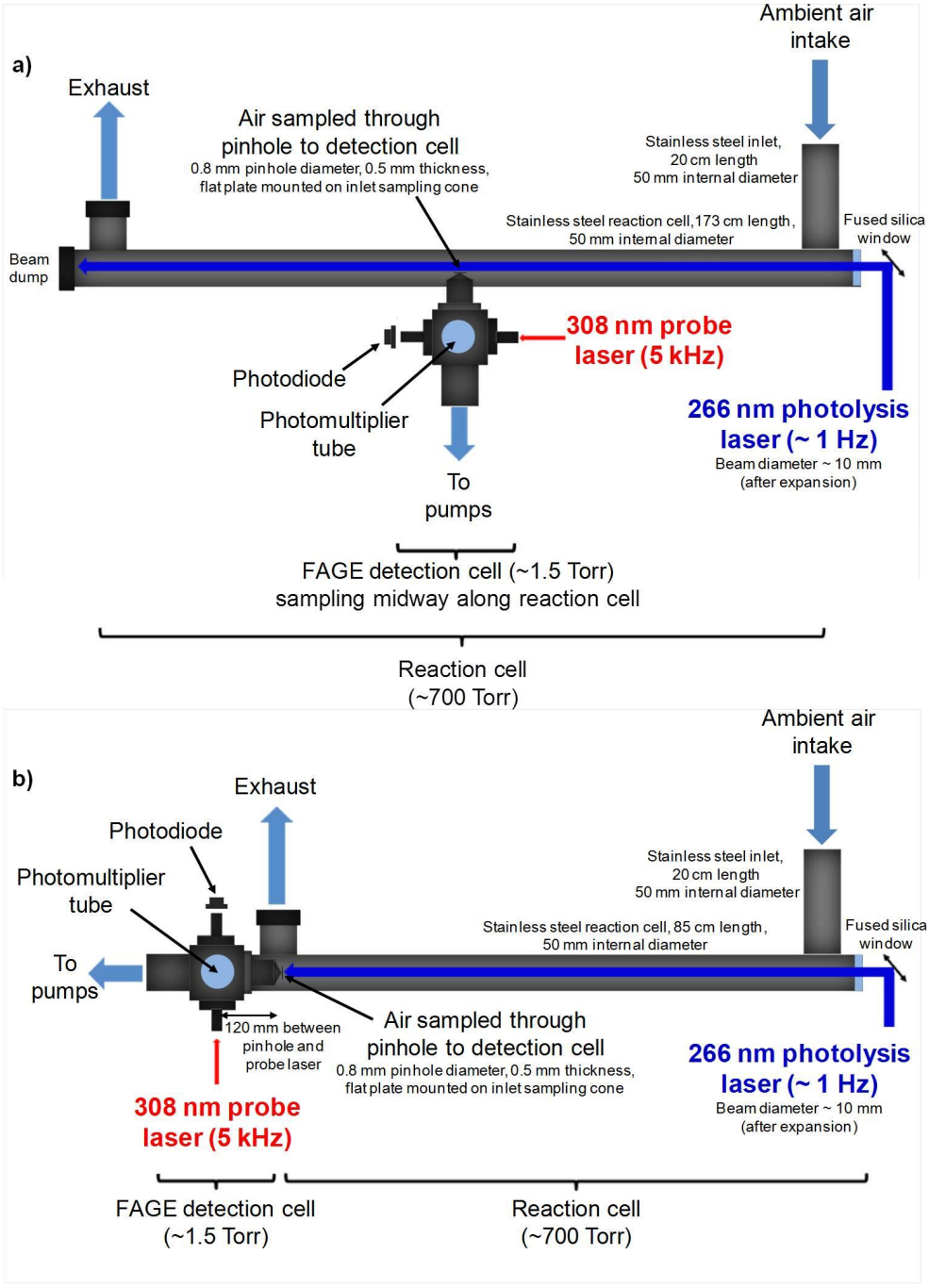

523

524 Figure 1: Schematic of the laser flash photolysis laser-induced fluorescence OH reactivity instrument for a)
525 experiments in which the FAGE detection cell was situated midway along the reaction cell, resulting in sampling at
526 90° to the air flow and leading to biexponential OH decays; b) experiments and field measurements in which the
527 FAGE detection cell was situated at the end of the reaction cell and sampled from the centre of the photolysed
528 volume, leading to OH decays described by a single exponential. All laboratory and field measurements shown in
529 this work were obtained with the instrument configuration as shown in panel (b).

Atmos. Meas. Tech. Discuss., doi:10.5194/amt-2016-51, 2016
Manuscript under review for journal Atmos. Meas. Tech.
Published: 29 February 2016

Atmospheric Measurement Techniques Discussions

530

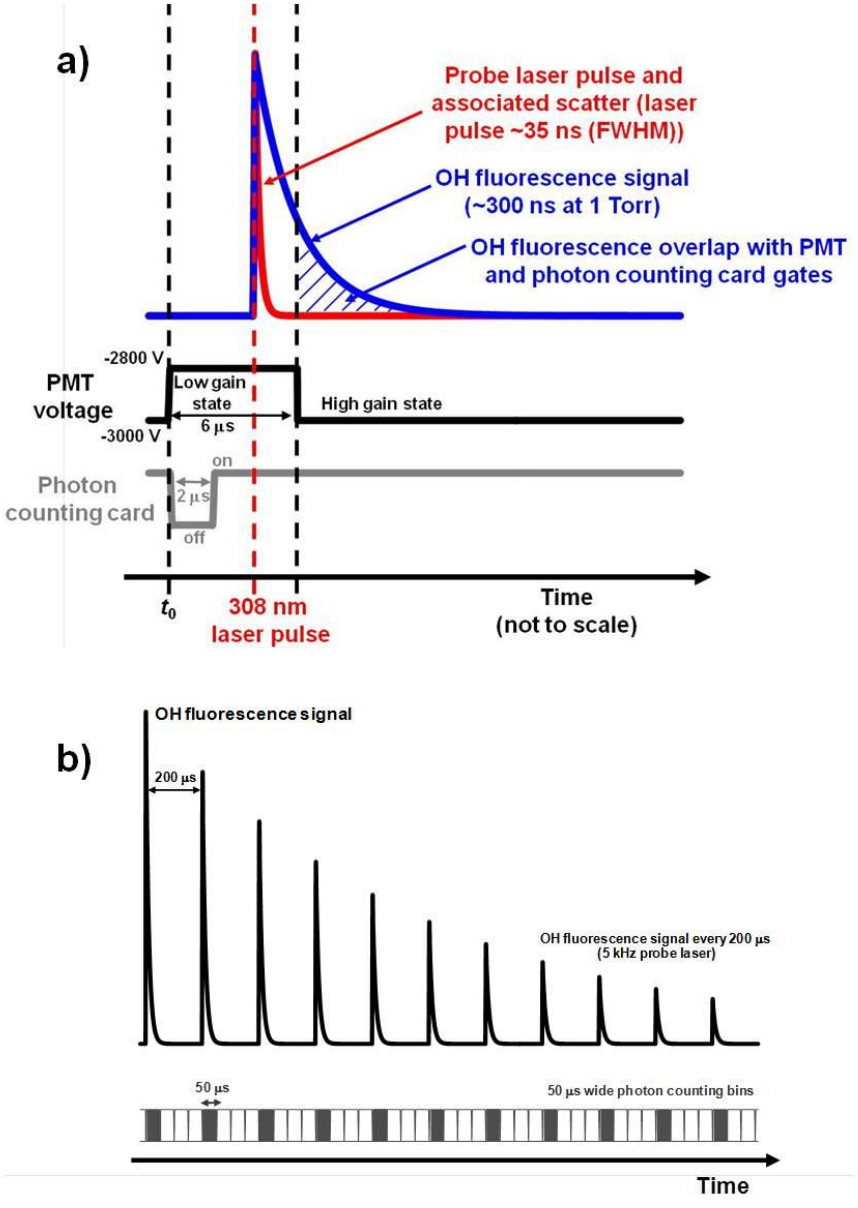

531

532 Figure 2: a) Schematic to illustrate the Stanford Research Systems delay generator controlled gate timing of the PMT
533 detector and photon counting card in the OH reactivity instrument. The blue hatched region indicates the overlap
534 between the OH fluorescence signal and the photon counting gates; b) Schematic to illustrate the photon counting
535 bin structure used to collect OH fluorescence photons after each 308 nm probe laser pulse (5kHz pulse repetition
536 frequency). Four 50 µs wide photon counting bins cover the time period between each 308 nm laser pulse, but only
537 the bins immediately after the laser pulse collect any fluorescence photons (shaded bins), and only the photon
538 counts from these bins are used to construct the OH decay.

Atmos. Meas. Tech. Discuss., doi:10.5194/amt-2016-51, 2016
Manuscript under review for journal Atmos. Meas. Tech.
Published: 29 February 2016

Atmospheric Measurement Techniques Discussions

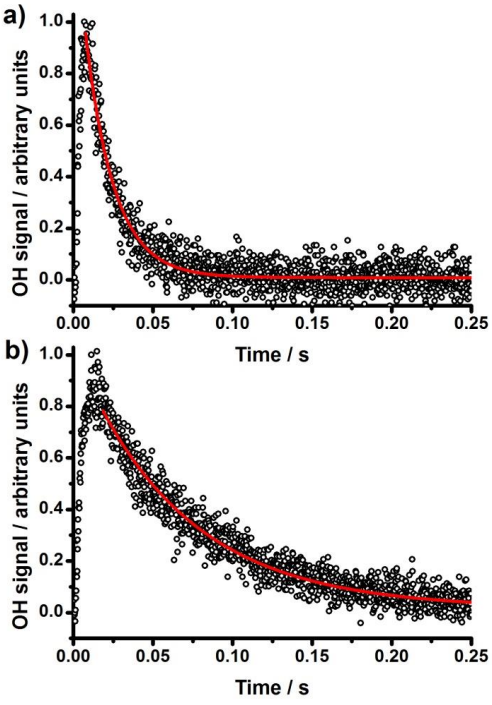

539

540 Figure 3: Typical OH time profiles following photolysis of ambient air (mixed with a small flow of $N_2/O_2/O_3/H_2O$)
541 observed during the Clean Air for London (ClearfLo) campaign (black points) with fits of Equation 6 (red lines) to the
542 LIF data to determine k'_{OH} for data recorded a) during a polluted period on 25th July 2012 (k'_{OH} = (46.6 ± 0.2) s^{-1}) and
543 b) during a cleaner period on 7th August 2012 (k'_{OH} = (13.9 ± 0.1) s^{-1}). Time zero is defined as the time at which
544 photolysis occurs. Decays represent data co-added throughout 5 min periods.

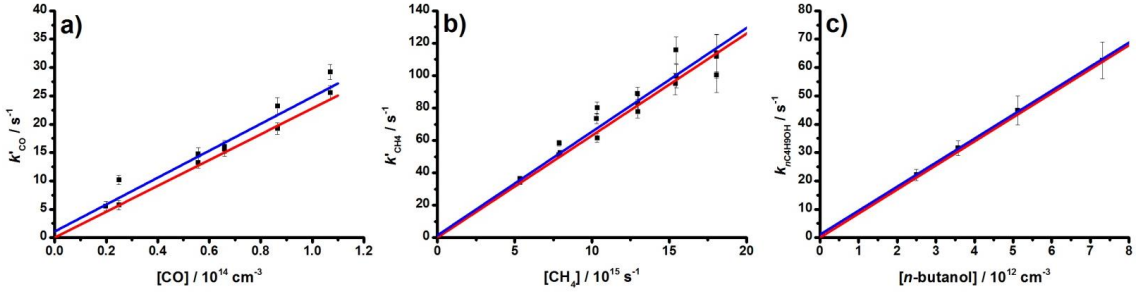

545

546 Figure 4: Bimolecular plots of pseudo-first-order rate coefficients describing OH loss (k'_{OH}) against known
547 concentrations of reactive gases during laboratory tests (black points) with best fit lines (blue) and literature values
548 (red) for a) CO at 298 K; b) CH_4 at 298 K; c) *n*-butanol (*n*-C_4H_9OH) in chamber experiments at 298 K. Literature values
549 are taken from Atkinson et al. (2004). Note that values for k_{phys} have been subtracted from the observed rate
550 coefficients describing OH loss (Equation 7), and corrections for dilution have been applied (Equation 8). Errors are
551 1σ.

Atmos. Meas. Tech. Discuss., doi:10.5194/amt-2016-51, 2016
Manuscript under review for journal Atmos. Meas. Tech.
Published: 29 February 2016

Atmospheric Measurement Techniques Discussions

552

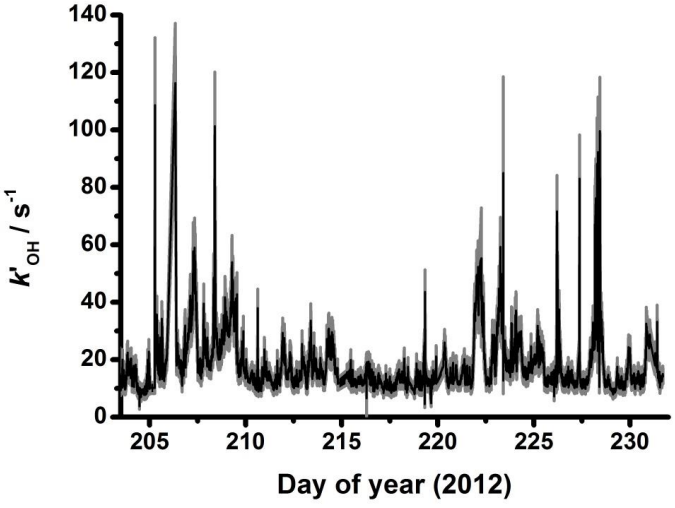

553

554 Figure 5: Time series of OH reactivity observed during the Clean Air for London (ClearfLo) campaign (21st July to 18th
555 August 2012). Uncertainties (represented by the shaded area) represent 1σ combined uncertainties from the fits to
556 observed OH decays (Equation 6), determinations of k_{phys} (Equation 7) and uncertainties in the dilution factor, f
557 (Equation 8).

558

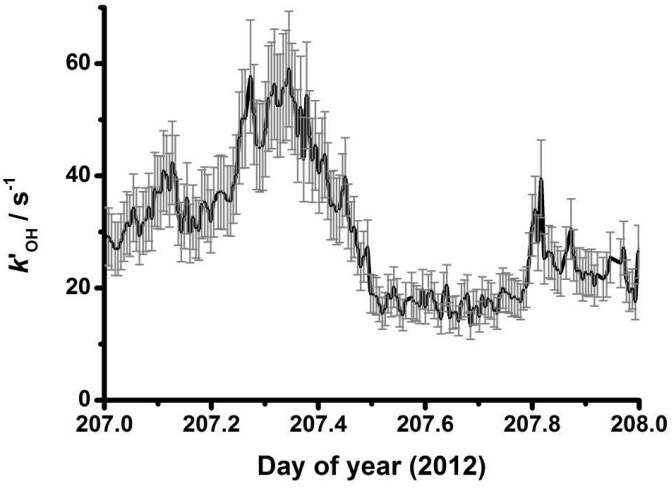

559

560 Figure 6: Time series of OH reactivity observed during the Clean Air for London (ClearfLo) campaign on the 25th July
561 2012 (Julian day 207). Error bars represent 1σ combined uncertainties from the fits to observed OH decays
562 (Equation 6), determinations of k_{phys} (Equation 7) and uncertainties in the dilution factor, f (Equation 8).

563

Atmos. Meas. Tech. Discuss., doi:10.5194/amt-2016-51, 2016
Manuscript under review for journal Atmos. Meas. Tech.
Published: 29 February 2016

Atmospheric Measurement Techniques Discussions

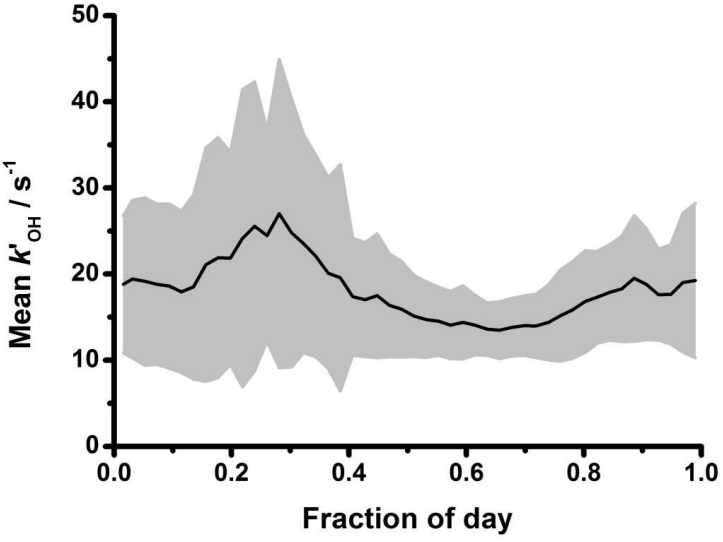

564

565 Figure 7: Diurnal average for observed OH reactivity (15 min averages) during the Clean Air for London (ClearfLo)
566 campaign (21st July to 18th August). Shaded areas represent the measurement variability from day-to-day during the
567 campaign.

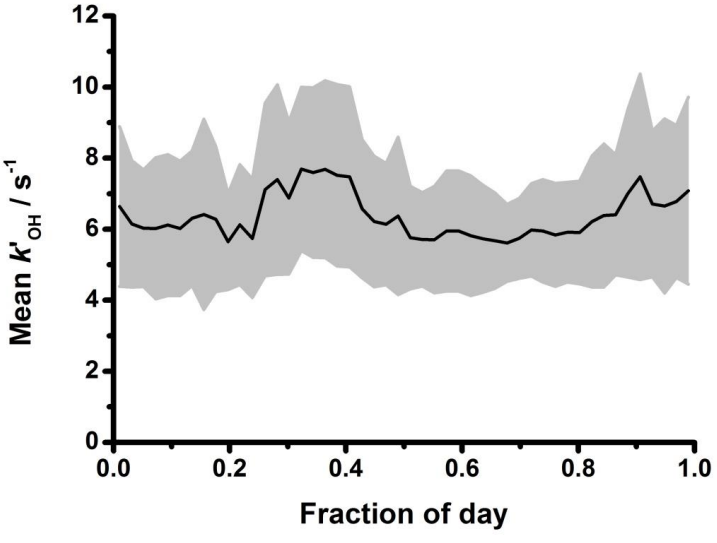

568

569 Figure 8: Diurnal average for observed OH reactivity (15 min averages) during in York (19th May to 16th June 2014).
570 Shaded areas represent the measurement variability from day-to-day.

571

Atmos. Meas. Tech. Discuss., doi:10.5194/amt-2016-51, 2016
Manuscript under review for journal Atmos. Meas. Tech.
Published: 29 February 2016

Atmospheric Measurement Techniques Discussions

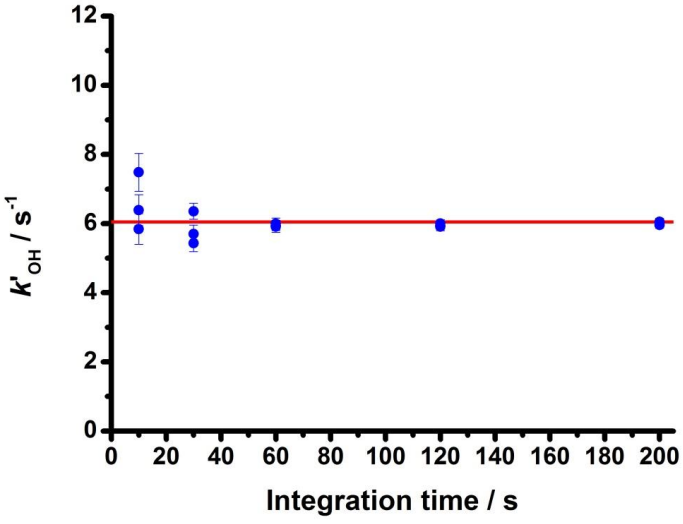

572

573 Figure 9: Observed OH reactivities, for a given gas composition (for which the expected OH reactivity is shown in
574 red), as a function of averaging time, obtained using 15 mW of 308 nm probe laser power.

575

576

577

578

579

580

581

Atmos. Meas. Tech. Discuss., doi:10.5194/amt-2016-51, 2016
Manuscript under review for journal Atmos. Meas. Tech.
Published: 29 February 2016

Atmospheric Measurement Techniques Discussions

582 **References**

583 Amedro, D., Miyazaki, K., Parker, A., Schoemaceker, C., and Fittschen, C.: Atmospheric and kinetic studies of OH and
584 HO_2 by the FAGE technique, J. Environ. Sci., 24, 1, 78-86, 2012

585 Atkinson, R., Baulch, D.L., Cox, R.A., Crowley, J.N., Hampson, R.F., Hynes, R.G., Jenkin, M.E., Rossi, M.J., and Troe, J.:
586 IUPAC Subcommittee for Gas Kinetic Data Evaluation, http://iupac.pole-ether.fr/, Atmos. Chem. Phys., 4, 1461-1738,
587 2004

588 Bloss, W.J., Gravestock, T.J., Heard, D.E., Ingham, T., Johnson, G.P., and Lee, J.D.: Application of a compact all solid-
589 state laser system to the in situ detection of atmospheric OH, HO_2, NO and IO by laser-induced fluorescence, J.
590 Environ. Monit., 5, 21–28, 2003

591 Bohnenstengel, S.I., Belcher, S.E., Aiken, A.C., Allan, J.D., Allen, G., Bacak, A., Bannan, T.J., Barlow, J.F., Beddows,
592 D.C.S., Bloss, W.J., Booth, A.M., Chemel, C., Coceal, O., Di Marco, C.F., Mavendra, D.K., Faloon, K.H., Fleming, Z.,
593 Furger, M., Gietl, J.K., Graves, R.R., Green, D.C., Grimmond, C.S.B., Halios, C., Hamilton, J.F., Harrison, R.M., Heal,
594 M.R., Heard, D.E., Helfter, C., Herndon, S.C., Holmes, R.E., Hopkins, J.R., Jones, A.M., Kelly, F.J., Kotthaus, S.,
595 Langford, B., Lee, J.D., Leigh, R., Lewis, A.C., Lidster, R.T., Lopez-Hilfiker, F., McQuaid, J.B., Mohr, C., Monks, P.S.,
596 Nemitz, E., Ng, N.L., Percival, C.J., Prévôt, A.S.H., Ricketts, H.M.A., Sokhi, R., Stone, D., Thornton, J.A., Tremper, A.H.,
597 Valach, A.C., Visser, S., Whalley, L.K., Williams, L.R., Xu, L., Young, D.E., and Zotter, P.: Meteorology, air quality, and
598 health in London: The ClearfLo project, Bull. Am. Meteor. Soc., 96, 5, 779-804, http://dx.doi.org/10.1175/BAMS-D-
599 12-00245.1, 2015

600 Cantrell, C.A., Shetter, R.E., Calvert, J.G., Eisele, F.L. and Tanner, D.J.: Some considerations of the origin of nighttime
601 peroxy radicals observed in MLOPEX, J. Geophys. Res.-Atmos., 102, 15899–15913, 1997

602 Chatani, S., Shimo, N., Matsunaga, S., Kajii, Y., Kato, S., Nakashima, Y., Miyazaki, K., Ishii, K., and Ueno, H.: Sensitivity
603 analyses of OH missing sinks over Tokyo metropolitan area in the summer of 2007, Atmos. Chem. Phys., 9, 8975–
604 8986, 2009

605 Commane, R., Floquet, C.F.A., Ingham, T., Stone, D., Evans, M.J., and Heard, D.E: Observations of OH and HO_2 radicals
606 over West Africa, Atmos. Chem. Phys., 10, 8783-8801, 2010

607 Creasey, D.J., Heard, D.E., and Lee, J.D.: Absorption Cross-section measurements of O_2 and H_2O at 185 nm.
608 Implications for the calibration of field instruments to measure OH, HO_2 and RO_2 radicals, Geophys. Res. Lett., 27,
609 1651-1654, 2000

610 Di Carlo, P., Brune, W.H., Martinez, M., Harder, H., Lesher, R., Ren, X., Thornberry, T., Carroll, M.A., Young, V.,
611 Shepson, P. B., Reimer, D., Apel, E., and Campbell, C.: Missing OH Reactivity in a Forest: Evidence for Unknown
612 Reactive Biogenic VOCs, Science, 304, 722–725, 2004

613 Dolgorouky, C., Gros, V., Sarda-Esteve, R., Sinha, V., Williams, J., Marchand, N., Sauvage, S., Poulain, L., Sciare, J., and
614 Bonsang, B.: Total OH reactivity measurements in Paris during the 2010 MEGAPOLI winter campaign, Atmos. Chem.
615 Phys., 12, 9593– 9612, doi:10.5194/acp-12-9593-2012, 2012

616 Edwards, P.M., Evans, M.J., Furneaux, K.L., Hopkins, J., Ingham, T., Jones, C., Lee, J.D., Lewis, A.C., Moller, S.J., Stone,
617 D., Whalley, L.K., and Heard, D.E.: OH reactivity in a South East Asian tropical rainforest during the Oxidant and
618 Particle Photochemical Processes (OP3) project, Atmos. Chem. Phys., 13, 9497–9514, doi:10.5194/acp-13-9497-
619 2013, 2013

620 Fuchs, H., Hofzumahaus, A., Rohrer, F., Bohn, B., Brauers, T., Dorn, H.-P., Haseler, R., Holland, F., Kaminski, M., Li, X.,
621 Lu, K., Nehr, S., Tillmann, R., Wegener, R., and Wahner, A.: Experimental evidence for efficient hydroxyl radical
622 regeneration in isoprene oxidation, Nature Geoscience, 6, 1023-1026, 2013

623 Glowacki, D.R., Goddard, A., Hemavibool, K., Malkin, T.L., Commane, R., Anderson, F., Bloss, W.J., Heard, D.E.,
624 Ingham, T., Pilling, M.J., and Seakins, P.W.: Design and initial results from a Highly Instrumented Reactor for
625 Atmospheric Chemistry, Atmos. Chem. Phys., 7, 20, 5371-5390, 2007

626 Hansen, R.F., Griffith, S.M., Dusanter, S., Rickly, P.S., Stevens, P.S., Bertman, S.B., Carroll, M.A., Erickson, M.H., Flynn,
627 J.H., Grossberg, N., Jobson, B.T., Lefer, B.L., and Wallace, H.W.: Measurements of total hydroxyl radical reactivity
628 during CABINEX 2009 – Part 1: Field measurements, Atmos. Chem. Phys., 14, 2923-2937, 2014

629 Ingham, T., Goddard, A., Whalley, L.K., Furneaux, K.L., Edwards, P.M., Seal, C.P., Self, D.E., Johnson, G.P., Read, K.A.,
630 Lee, J.D., and Heard, D.E.: A flow-tube based laser-induced fluorescence instrument to measure OH reactivity in the
631 troposphere, Atmos. Meas. Tech., 2, 465–477, 2009

632 Kim, S., Guenther, A., Karl, T., and Greenberg, J.: Contributions of primary and secondary biogenic VOC tototal OH
633 reactivity during the CABINEX (Community Atmosphere-Biosphere INteractions Experiments)-09 field campaign,
634 Atmos. Chem. Phys., 11, 8613–8623, doi:10.5194/acp-11-8613-2011, 2011

635 Kovacs, T.A. and Brune, W.H.: Total OH Loss Rate Measurement, J. Atmos. Chem., 39, 105–122, 2001

636 Kovacs, T.A., Brune, W.H., Harder, H., Martinez, M., Simpas, J.B., Frost, G.J., Williams, E., Jobson, T., Stroud, C.,
637 Young, V., Fried, A., and Wert, B.: Direct measurements of urban OH reactivity during Nashville SOS in summer 1999,
638 J. Environ. Monitor., 5, 68–74, 2003

639 Lee, J.D., Young, J.C., Read, K.A., Hamilton, J.F., Hopkins, J.R., Lewis, A.C., Bandy, B.J., Davey, J., Edwards, P., Ingham,
640 T., Self, D.E., Smith, S.C., Pilling, M.J., and Heard, D.E.: Measurement and calculation of OH reactivity at a United
641 Kingdom coastal site, J. Atmos. Chem., 64, 53–76, 2009

642 Lou, S., Holland, F., Rohrer, F., Ku, K., Bohn, B., Brauers, T., Chang, C.C., Fuchs, H., Haseler, R., Kita, K., Kondo, Y., Li,
643 X., Shao, M., Zeng, L., Wahner, A., Zhang, Y., Wang, W., and Hofzumahaus, A.: Atmospheric OH reactivities in the
644 Pearl River Delta – China in summer 2006: measurements and model results, Atmos. Chem. Phys., 10, 11243-11260,
645 2010

646 Lu, K.D., Hofzumahaus, A., Holland, F., Bohn, B., Brauers, T., Fuchs, H., Hu, M., Haseler, R., Kita, K., Kondo, Y., Li, X.,
647 Lou, S.R., Oebel, A., Shao, M., Zeng, L.M., Wahner, A., Zhu, T., Zhang, Y.H., and Rohrer, F.: Missing OH source in a
648 suburban environment near Beijing: observed and modelled OH and HO_2 concentrations in summer 2006, Atmos.
649 Chem. Phys., 13, 1057-1080, 2013

650 Malkin, T.L., Goddard, A., Heard, D.E., and Seakins, P.W.: Measurements of OH and HO_2 yields from the gas phase
651 ozonolysis of isoprene, Atmos. Chem. Phys., 10, 3, 1441-1459, 2010

652 Mao, J., Ren, X., Brune, W.H., Olson, J.R., Crawford, J.H., Fried, A., Huey, L.G., Cohen, R.C., Heikes, B., Singh, H.B.,
653 Blake, D.R., Sachse, G.W., Diskin, G.S., Hall, S.R., and Shetter, R.E.: Airborne measurement of OH reactivity during
654 INTEX-B, Atmos. Chem. Phys., 9, 163–173, 2009

655 Mao, J., Ren, X., Chen, S., Brune, W.H., Chen, Z., Martinez, M., Harder, H., Lefer, B., Rappenglück, B., Flynn, J., and
656 Leuchner, M.: Atmospheric oxidation capacity in the summer of Houston 2006: Comparison with summer
657 measurements in other metropolitan studies, Atmos. Environ., 44, 4107–4115, 2010

658 Martinez, M., Harder, H., Kovacs, T.A., Simpas, J.B., Bassis, J., Lesher, R., Brune, W.H., Frost, G.J., Williams, E.J.,
659 Stroud, C.A., Jobson, B.T., Roberts, J.M., Hall, S.R., Shetter, R.E., Wert, B., Fried, A., Alicke, B., Stutz, J., Young, V.L.,
660 White, A.B., and Zamora, R.J.: OH and HO_2 concentrations, sources, and loss rates during the Southern Oxidants
661 Study in Nashville, Tennessee, summer 1999, J. Geophys. Res. Atmos., 108, D19, 4617, 1-17,
662 doi:10.1029/2003JD003551, 2003

663 Michoud, V., Hansen, R.F., Locoge, N., Stevens, P.S., and Dusanter: Detailed characterizations of the new Mines
664 Douai comparative reactivity method instrument via laboratory experiments and modelling: Atmos. Meas. Tech., 8,
665 3537-3553, doi:10.5194/amt-8-3537-2015, 2015

666 Mogensen, D., Smolander, S., Sogachev, A., Zhou, L., Sinha, V., Guenther, A., Williams, J., Nieminen, T., Kajos, M. K.,
667 Rinne, J., Kulmala, M., and Boy, M.: Modelling atmospheric OH-reactivity in a boreal forest ecosystem, Atmos. Chem.
668 Phys., 11, 9709– 9719, doi:10.5194/acp-11-9709-2011, 2011

669 Nakashima, Y., Kamei, N., Kobayashi, S., and Kajii, Y.: Total OH reactivity and VOC analyses for gasoline vehicular
670 exhaust with a chassis dynamometer, Atmos. Environ., 44, 4, 468-475, 2010

671 Nakashima, Y., Tsurumaru, H., Imamura, T., Bejan, I., Wenger, J.C., and Kajii, Y.: Total OH reactivity measurements in
672 laboratory studies of the photooxidation of isoprene, Atmos. Environ., 62, 243-247, 2012

673 Nakashima, Y., Kato, S., Greenberg, J., Harley, P., Karl, T., Turnipseed, A., Apel, E., Guenther, A., Smith, J., and Kajii, Y.:
674 Total OH reactivity measurements in ambient air in a southern Rocky mountain ponderosa pine forest during
675 BEACHON-SRM08 summer campaign, Atmos. Environ., 85, 1-8, 2014

676 Nölscher, A.C., Williams, J., Sinha, V., Custer, T., Song, W., Johnson, A.M., Axinte, R., Bozem, H., Fischer, H., Pouvesle,
677 N., Phillips, G., Crowley, J.N., Rantala, P., Rinne, J., Kulmala, M., Gonzales, D., Valverde-Canossa, J., Vogel, A.,
678 Hoffmann, T., Ouwersloot, H.G., Vilà-Guerau de Arellano, J., and Lelieveld, J.: Summertime total OH reactivity
679 measurements from boreal forest during HUMPPA-COPEC 2010, Atmos. Chem. Phys., 12, 8257–8270,
680 doi:10.5194/acp-12-8257-2012, 2012

681 Nolscher, A.C., Butler, T., Auld, J., Veres, P., Munoz, A., Taraborrelli, D., Vereecken, L., Leliveld, J., and Williams, J.:
682 Using total OH reactivity to assess isoprene photooxidation via measurement and model, Atmos. Environ., 89, 453-
683 463, 2014

684 Parker, A.E., Amedro, D., Schoemaecker, C., and Fittschen, C.: OH radical reactivity measurements by FAGE, Environ.
685 Eng. and Management J., 10, 1, 107-114, 2011

686 Ren, X., Harder, H., Martinez, M., Lesher, R.L., Oliger, A., Shirley, T., Adams, J., Simpas, J.B., and Brune, W.H.: HO_x
687 concentrations and OH reactivity observations in New York City during PMTACS-NY2001, Atmos. Environ., 37, 3627–
688 3637, 2003

689 Ren, X., Brune, W.H., Mao, J.Q., Mitchell, M.J., Lesher, R.L., Simpas, J.B., Metcalf, A.R., Schwab, J.J., Cai, C.X., Li, Y.Q.,
690 Demerjian, K.L., Felton, H.D., Boynton, G., Adams, A., Perry, J., He, Y., Zhou, X. L., and Hou, J.: Behavior of OH and
691 HO_2 in the winter atmosphere in New York city, Atmos. Environ., 40, 252–263, 2006a

692 Ren, X., Brune, W.H., Oliger, A., Metcalf, A.R., Simpas, J.B., Shirley, T., Schwab, J.J., Bai, C., Roychowdhury, U., Li, Y.,
693 Cai, C., Demerjian, K.L., He, Y., Zhou, X., Gao, H., and Hou, J.: OH, HO_2, and OH reactivity during the PMTACS-NY
694 Whiteface Mountain 2002 campaign: Observations and model comparison, J. Geophys. Res., 111, D10S03,
695 doi:10.1029/2005JD006126, 2006b

696 Sadanaga, Y., Yoshino, A., Watanabe, K., Yoshioka, A., Wakazono, Y., Kanaya, Y., and Kajii, Y.: Development of a
697 Measurement System of OH reactivity in the atmosphere using a laser-induced pump and probe technique, Rev. Sci.
698 Instrum., 75, 2648– 2655, 2004a

699 Sadanaga, Y., Yoshino, A., Kato, S., Yoshioka, A., Watanabe, K., Miyakawa, Y., Hayashi, I., Ichikawa, M., Matsumoto,
700 J., Nishiyama, A., Akiyama, N., Kanaya, Y., and Kajii, Y.: The importance of NO_2 and volatile organic compounds in the
701 urban air from the viewpoint of the OH reactivity, Geophys. Res. Lett., 31, L08102, doi:10.1029/2004gl019661,
702 2004b

703 Shirley, T.R., Brune, W.H., Ren, X., Mao, J., Lesher, R., Cardenas, B., Volkamer, R., Molina, L.T., Molina, M.J., Lamb, B.,
704 Velasco, E., Jobson, T., and Alexander, M.: Atmospheric oxidation in the Mexico City Metropolitan Area (MCMA)
705 during April 2003, Atmos. Chem. Phys., 6, 2753-2765, 2006

706 Sinha, V., Williams, J., Crowley, J.N., and Lelieveld, J.: The Comparative Reactivity Method – a new tool to measure
707 total OH Reactivity in ambient air, Atmos. Chem. Phys., 8, 2213–2227, 2008

708 Sinha, V., Williams, J., Diesch, J.M., Drewnick, F., Martinez, M., Harder, H., Regelin, E., Kubistin, D., Bozem, H.,
709 HosaynaliBeygi, Z., Fischer, H., Andrés-Hernández, M.D., Kartal, D., Adame, J.A., and Lelieveld, J.: Constraints on
710 instantaneous ozone production rates and regimes during DOMINO derived using in-situ OH reactivity
711 measurements, Atmos. Chem. Phys., 12, 7269–7283, doi:10.5194/acp-12-7269-2012, 2012

712 Stone, D., Blitz, M., Ingham, T., Onel, L., Medeiros, D.J. and Seakins, P.W.: An instrument to measure fast gas phase
713 radical kinetics at high temperatures and pressures, submitted 2016

714 Whalley, L.K., Furneaux, K.L., Goddard, A., Lee, J.D., Mahajan, A., Oetjen, H., Read, K.A., Kaaden, N., Carpenter, L. J.,
715 Lewis, A. C., Plane, J. M. C., Saltzman, E. S., Wiedensohler, A., and Heard, D. E.: The chemistry of OH and HO_2 radicals
716 in the boundary layer over the tropical Atlantic Ocean, Atmos. Chem. Phys., 10, 1555–1576, 2010

717 Whalley, L.K., Edwards, P.M., Furneaux, K.L., Goddard, A., Ingham, T., Evans, M.J., Stone, D., Hopkins, J.R., Jones, C.E.,
718 Karunaharan, A., Lee, J.D., Lewis, A.C., Monks, P.S., Moller, S.J., and Heard, D.E.: Quantifying the magnitude of a
719 missing hydroxyl radical source in a tropical rainforest, Atmos. Chem. Phys., 11, 7223-7233, 2011

720 Whalley, L.K., Stone, D., Bandy, B., Dunmore, R., Hamilton, J.F., Hopkins, J., Lee, J.D., Lewis, A.C., and Heard, D.E.:
721 Atmospheric OH reactivity in central London: observations, model predictions and estimates of in-situ ozone
722 production, Atmos. Chem. Phys. Discuss., 15, 31247-31286, 2015

723 Winiberg, F.A.F., Smith, S.C., Bejan, I., Brumby, C.A., Ingham, T., Malkin, T.L., Orr, S.C., Heard, D.E., and Seakins, P.W.:
724 Pressure-dependent calibration of the OH and HO_2 channels of a FAGE HO_x instrument using the Highly Instrumented
725 Reactor for Atmospheric Chemistry (HIRAC), Atmos. Meas. Tech., 8, 2, 523-540, 2015

726 Yoshino, A., Sadanaga, Y., Watanabe, K., Kato, S., Miyakawa, Y., Matsumoto, J., and Kajii, Y.: Measurement of total
727 OH reactivity by laser-induced pump and probe technique – comprehensive observations in the urban atmosphere
728 of Tokyo, Atmos. Environ., 40, 7869–7881, 2006

729 Yoshino, A., Nakashima, Y., Miyazaki, K., Kato, S., Suthawaree, J., Shimo, N., Matsunaga, S., Chatani, S., Apel, E.,
730 Greenberg, J., Guenther, A., Ueno, H., Sasaki, H., Hoshi, J., Yokota, H., Ishii, K., and Kajii, Y.: Air quality diagnosis from
731 comprehensive observations of total OH reactivity and reactive trace species in urban central Tokyo, Atmos.
732 Environ., 49, 51-59, 2012

733